Oxygen Reduction Reaction (ORR) of Pt/C Standard in Different Electrolyte Solutions and Terbium(III) Monoporphyrinato Complex

Atmanto Heru Wibowo[1*], Annisa Nur Buana Wati[1], Anas Santria[2,3], Abu Masykur[1], and Maulidan Firdaus[1]

[1]*Department of Chemistry, Faculty of Natural Sciences and Mathematics, Universitas Sebelas Maret, Jl. Ir. Sutami 36A, Kentingan, Surakarta 57126, Indonesia*

[2]*Department of Chemistry, Graduate School of Science, Osaka University, Toyonaka, Osaka 560-0043, Japan*

[3]*Research Center for Chemistry, National Research and Innovation Agency (BRIN), Serpong 15314, Indonesia*

* ***Corresponding author:***

tel: +62-85878677541
email: aheruwibowo@staff.uns.ac.id

Received: November 2, 2022
Accepted: March 22, 2023

DOI: 10.22146/ijc.78807

Abstract: *Electrocatalytic parameters of a Pt/C standard and a sample of terbium(III) monoporphyrinato were investigated in different solutions. N electron transfer, Tafel slope, E_{onset}, and overpotential of the catalyst of Pt/C in different solutions were calculated and analyzed using a rotating ring disk electrode (RRDE) in 0.5 M H_2SO_4, 0.1 M $HClO_4$ and 0.1 M NaOH. In the RRDE measurements, a bipotentiostat at a potential range of 1.03 to 0.05 V vs RHE (E_{ring} = 1.2 V vs RHE) with a scan rate of 5 mV/s and rotation rates of 200, 400, 900, 1600 and 2500 rpm was used. Hereafter, the test of terbium(III) monoporphyrinato compound formulated in [Tb(TPP)(cyclen)]Cl (TPP = 5,10,15,20-tetraphenylporphyrinato; cyclen = 1,4,7,10-tetraazacyclododecane) as a candidate material for ORR electrocatalyst was also done. The results showed that the measurement of Pt/C standards was satisfactory according to the literature for all parameters with the n electron transfer close to 4 in all electrolytes media. [Tb(TPP)(cyclen)]Cl had an n electron transfer value of 2.38, suggesting that the [Tb(TPP)(cyclen)]Cl compound has less potential for ORR catalysts.*

Keywords: *oxygen reduction reaction (ORR); RRDE technique; Pt/C; monoporphyrinato*

■ INTRODUCTION

The fuel cell is one of the options to obtain promising energy in the future. However, the kinetic sluggishness on the cathode and high overpotential is the main problem that is mostly found in the fuel cell, especially for oxygen reduction reactions (ORR). Therefore, high efficiency is required in the oxygen reduction process that occurs on the cathode and is inevitable in the polymer electrolyte membrane fuel cells (PEMFC). PEMFC affords high efficiency of the fuel cell in supplying electricity with nearly nonexistent emission [1]. For a PEMFC that uses a Pt electrode, the ORR occurred in the cathode and the hydrogen oxidation reaction (HOR) occurred in the anode [2]. Because the nature of ORR being a kinetically slow reaction with high overpotential, an efficient electrocatalyst is necessary [3]. However, Pt is still used mostly for ORR due to its good catalytic activity compared to other materials. A significant portion of the high cost of PEMFCs was contributed due to the price of Pt-based catalysts [4]. Therefore, it is important to design an electrocatalyst that is cheap and efficient for ORR [5].

The potential candidate to replace Pt are precursors containing nitrogen, carbon, and metals [6]. Molecules of N4-metallomacrocyclic have been considered as one of the promising compounds for ORR since 1964. The advantage of using these materials for electrocatalysts is due to the more affordable price compared to Pt. Catalytic activity can be modified by changing the substitution of the metal center or by the structure modification of N4-macrocyclic ligand [7].

Porphyrin, corrole, and phthalocyanine have been studied extensively regarding the substituent effect for the catalyst of ORR [8]. The use of metals on porphyrin (henceforth called metalloporphyrin) showed some benefits from the aspect of its coordination. Porphyrin affords rigid environments and good stability with the metal center in the cavity. Metalloporphyrin is considered as a stable complex in acid or base, and is also a redox-active compound. As a consequence, metalloporphyrin can be used for redox activity materials such as in the applications for fuel cells. The porphyrin molecule can be modified with different substituents on the *meso* and β position to obtain various metalloporphyrin with different chemical or physico-chemical properties that can also be applied for the ORR catalyst [9]. A metalloporphyrin complex with a lanthanide ion as a metal center has also contributed to porphyrin chemistry since 1974, in which the study of this complex has been done in many aspects such as photoluminescence and molecular magnetism [10].

An electrocatalyst performance should be evaluated first before involving the fabrication of the fuel cell in the lab using a three-electrode system [11]. Evaluation can be done using a rotating disk electrode (RDE) and rotating-ring-disk electrode (RRDE) as the working electrode in the system. The Pt/C electrocatalyst has been used as a reference material for evaluating the performance of new catalysts, which is dependent on some factors [12]. Here we report the determination of the catalytic activity of platinum in different electrolyte media, together with an investigation of the catalytic performance of lanthanide(III) monoporphyrinato complex, namely [Tb(TPP)(cyclen)]Cl (Tb = terbium; TPP = 5,10,15,20-tetraphenylporphyrinato; cyclen = 1,4,7,10-tetraazacyclododecane; Cl = chloride).

■ EXPERIMENTAL SECTION

Materials

[Tb(TPP)(cyclen)]Cl complex was prepared using the previously reported method [10]. The Pt/C (20 wt.% Pt), Sulfuric Acid (H_2SO_4, 97%), perchloric acid ($HClO_4$, 96%), sodium hydroxide (NaOH), isopropanol (C_3H_8O) and Nafion 5 wt.% were purchased from commercial suppliers, E Merk and DuPont.

Instrumentation

The RRDE measurements were carried out using bipotentiostat Corrtest CS2150 from Corrtest Instruments Corp., Ltd. with the current control range: ± 2 A. The computational chemistry calculations were done using Supercomputer System SQUID at the Cybermedia Centre, Osaka University.

Procedure

The electrocatalytic activities of catalysts were studied using RRDE measurement in a three-electrode cell. A Pt/GC RRDE (7 mm OD, 5 mm ID Pt ring (0.189 cm^2) and 4 mm diameter GC (0.126 cm^2), Ag/AgCl (sat. KCl) and GC plate (10 × 15 mm, 2 mm thickness, connected with Au wire) were used as the working, reference and counter electrode, respectively. The ink catalyst was prepared by mixing 2 mg of catalyst and 1 mL stock solution (20% isopropanol, 0.02% Nafion ionomer), followed by sonification for about 60 min. About 10 µL of dispersed ink was drop cast on the surface of the GC-electrode disk and then air-dried for about 60 min. The RRDE measurements were carried out at +1.03 to +0.05 V vs RHE (E_{ring} = 1.2 V vs RHE) with the rotating rate of 200, 400, 900, 1600, and 2500 rpm and a scan rate of 10 mV s^{-1} in the 0.1 M KOH solution.

Computational chemistry calculations was performed on the Gaussian 16 package, Rev. C.01. The geometry structure of $[Tb(TPP)cyclen]^+$ was taken from the experimental structure [10]. The Grimme's density functional theory (DFT-D3) method of B3LYP with the energy-consistent pseudopotentials of the Stuttgart (Stuttgart RSC 1997 ECP) basis set for terbium ion and 6-31G** basis set for the other atoms was performed to optimize the geometry of structure [13-15].

■ RESULTS AND DISCUSSION

Pt/C test in Various Electrolytes

The polarization curve was obtained with the linear sweep voltammetry (LSV) from RRDE at the range of 1.03 to 0.05 V vs RHE with scanning rates of 5 mV/s and rotation rates of 200, 400, 900, 1600 and 2500 rpm for Pt/C in various O_2 saturated solution of H_2SO_4 0.5 M, $HClO_4$ 0.1 M and NaOH 0.1 M. Current

obtained from the measurement was normalized with the disk surface (S_g) at about 0.126 cm^2. The profile of the Pt/C voltammetry in the various O_2 saturated solution (Fig. 1) showed that the current density increased with the increase of rotation rate from 200 to 2500 rpm. Table 1 shows the parameter analyzed from polarization curves at 2500 rpm. Analysis of the activation area (AR) of the polarization curve at 2500 rpm made it possible to obtain the parameter of E_{onset} value. More positive E_{onset} and $E_{1/2}$ means that the electrocatalysis will be more active [16]. The Pt/C catalyst in the medium of $HClO_4$ 0.1 M and NaOH 0.1 M showed more positive E_{onset} value than in H_2SO_4 0.1 M, indicating that Pt/C was more active in both solutions. The controlled region that was measured was in the mixed region of diffusion-kinetic (KR) to obtain information about $E_{1/2}$. The $E_{1/2}$ value was in the same correlation with the electrocatalytic activity of Pt/C in various electrolyte solutions of NaOH 0.1 M > $HClO_4$ 0.1 > H_2SO_4 0.5 M. The theory of the overpotential (η) and real overpotential (η_{exp}) was calculated from the different values of $E_{eq(exp)}$ and E_{onset} with E_{eq}. The difference of both overpotentials was used in the calculation of the sluggishness of ORR, where Pt/C in $HClO_4$ 0.1 M solution obtained the best value among other solutions.

From Eq. (1), the Koutecky-Levich plot is defined as a straight line characterized by the slope $\alpha_{K\text{-}L} = (n_{ex}B)^{-1}$ and the intercept $\beta_{K\text{-}L} = j_k^{-1}$ where j is the measured current density, j_k is the kinetic current density, j_l^{film} is the diffusion-limiting current density in catalyst film, j_l^{ads} is the diffusion-limiting current density associated with O_2 adsorption in the active site, j_0 is the current exchange density, n_{ex} is the exchange number of electrons, Ω is the rotation rate, θ and θ_{eq} is the degree of coverage of the catalyst surface (active sites) by oxygen at potential E, and at the equilibrium potential E_{eq}, η is the overpotential and b is the Tafel slope. The plot of Koutecky-Levich for Pt/C in various electrolyte solutions at different potentials showed a good linearity of the lines (Fig. 2). Typical

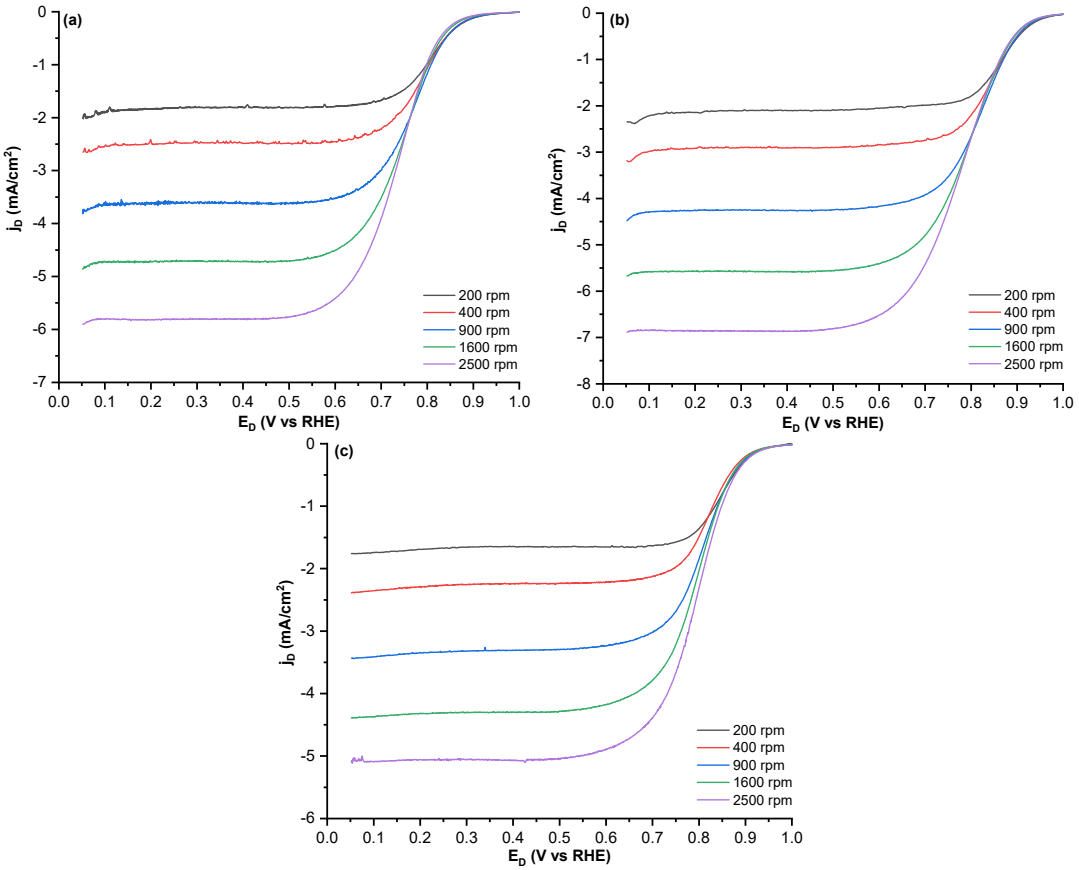

Fig 1. Polarization curve of Pt/C in various electrolyte solutions of (a) H_2SO_4 0.5 M, (b) $HClO_4$ 0.1 M and (c) NaOH 0.1 M at various rotation rates

Table 1. Parameters of the polarization curves for Pt/C in various electrolytes

Electrolyte	E_{onset} (V vs RHE)	$E_{1/2}$ (V vs RHE)	η (mV)	$η_{(exp)}$ (mV)	Sluggishness (mV)
0.5 M H_2SO_4	0.84	0.74	264	348	84
0.1 M $HClO_4$	0.89	0.78	232	291	59
0.1 M NaOH	0.89	0.80	167	296	129

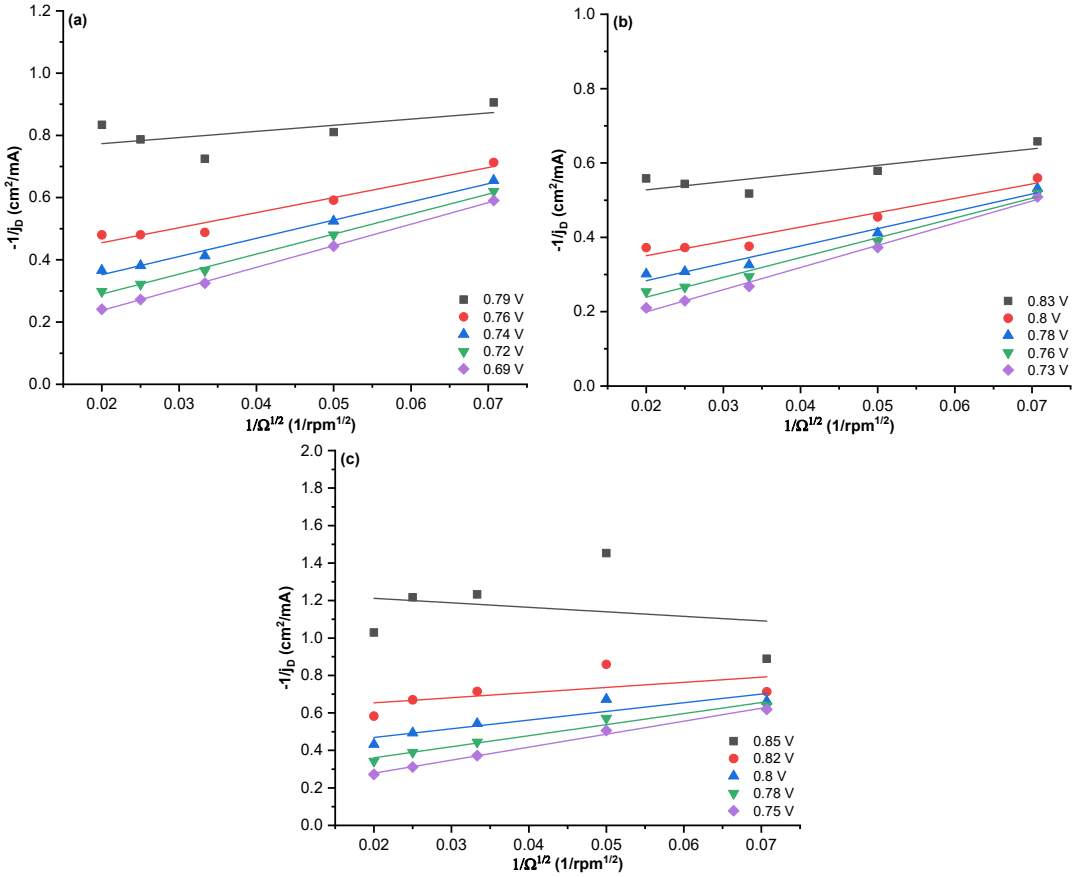

Fig 2. Koutecky-Levich plot obtained from Fig. 1 for Pt/C in the O_2 saturated solution of (a) H_2SO_4 0.5 M, (b) $HClO_4$ 0.1 M and (c) NaOH 0.1 M at the different potentials

characteristics of first-order kinetics in correlation with dissolved O_2 in the solution were seen with linearity and parallelism of the plots [17]. Kinetic current density (j_k) was normalized with the mass of Pt/C, which was drop-casted on the disk surface (20 μg). The value of j_k at 0.8 V vs RHE for the activation of Pt/C in various electrolytes is shown in Table 2.

$$\frac{1}{j}=\frac{1}{n_{ex}B\Omega^{\frac{1}{2}}}+\frac{1}{j_l^{film}}+\frac{1}{j_l^{ads}}+\frac{1}{j_0\frac{\theta}{\theta_{eq}}e^{\frac{n}{b}}}\Rightarrow j^{-1} \quad (1)$$

$$=(nexB)^{-1}\Omega^{-\frac{1}{2}}+j_k^{-1}$$

Fig. 3 shows plots based on Eq. (2), in which j_L (limiting current density) can be determined from these extrapolation plots. The j_L value for Pt/C in various electrolytes can be seen in Table 2. The j_L is always higher than j_0, independent of the solution used. This indicated that electron transfer is the determining stage for the reaction rate (rds) [18].

$$\frac{1}{j_k}=\frac{1}{j_L}+\frac{1}{j_0\frac{\theta}{\theta_{eq}}e^{\frac{\eta}{b'}}}=\frac{1}{jL}+\frac{1}{j_0\frac{\theta}{\theta_{eq}}e^{-\frac{E-E_{eq}}{b'}}}\Rightarrow\lim_{\eta\to\infty}\left(\frac{1}{j_k}\right) \quad (2)$$

$$=\frac{1}{j_L}$$

Table 2. ORR kinetic parameter of Pt/C in various solutions

Electrolyte	n	j_k (mA/cm²mg) at 0.8 V vs RHE	j_L (mA/cm²)	B (mV/dec)	j_0 (mA/cm²)
0.5 M H_2SO_4	3.95	52.74	62.35	114	5.52×10^{-4}
0.1 M $HClO_4$	3.99	183.02	61.57	112	1.42×10^{-3}
0.1 M NaOH	3.98	132.79	32.03	134	4.92×10^{-3}

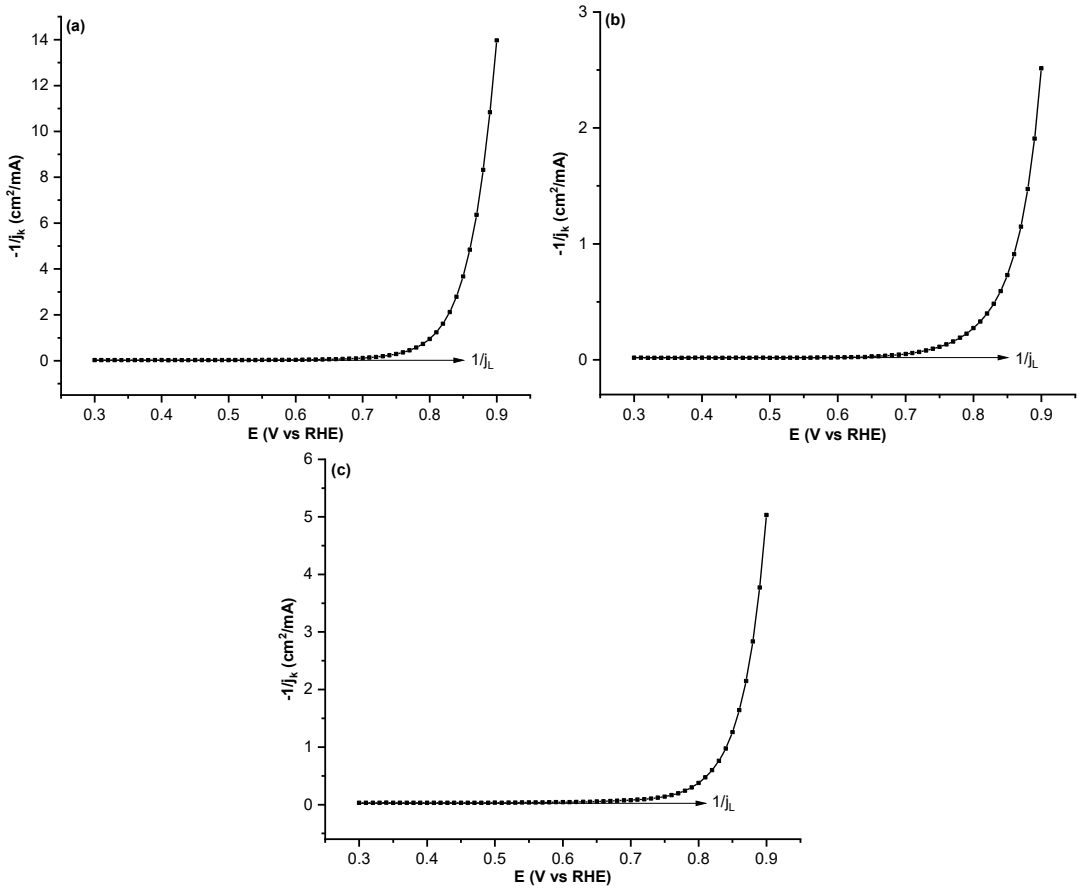

Fig 3. Plot "j_k^{-1} vs. E" for the determination of the limiting current density (j_L) for Pt/C in the electrolyte solution of (a) H_2SO_4 0.5 M, (b) $HClO_4$ 0.1 Mand (c) NaOH 0.1 M

Fig. 4 shows the relative Tafel plot of Pt/C in various electrolyte solutions. This plot can give information about the value of the Tafel slope (b) and exchange current density (j_0) obtained from Eq. (3) and (4), respectively, as seen in Table 2. From this calculation, the b value obtained was close to the literature with a high overpotential of about 120 mV/dec [19], indicating that the first electron reduction occurred as rds at high overpotential. Electrocatalytic material with high j_0 and low b is intended for electrocatalysis of ORR. This means that with lower b, the current density increases but with smaller overpotential, and it also means that the kinetic charge transfer occurred faster.

$$\alpha_{Tafel} = \frac{\partial \eta}{\partial\left(\log\left(\frac{j_k}{j_L - j_k}\right)\right)} = -b \quad (3)$$

$$\beta_{Tafel} = -b\log\left(\frac{j_L}{j_0}\right) \Rightarrow j_0 = j_L \times 10^{-\frac{\beta_{Tafel}}{b}} \quad (4)$$

The polarization curve of RRDE (Fig. 5) showed the currents on the disk and ring as well. The ring current (I_R) was parallel with the number of intermediate species

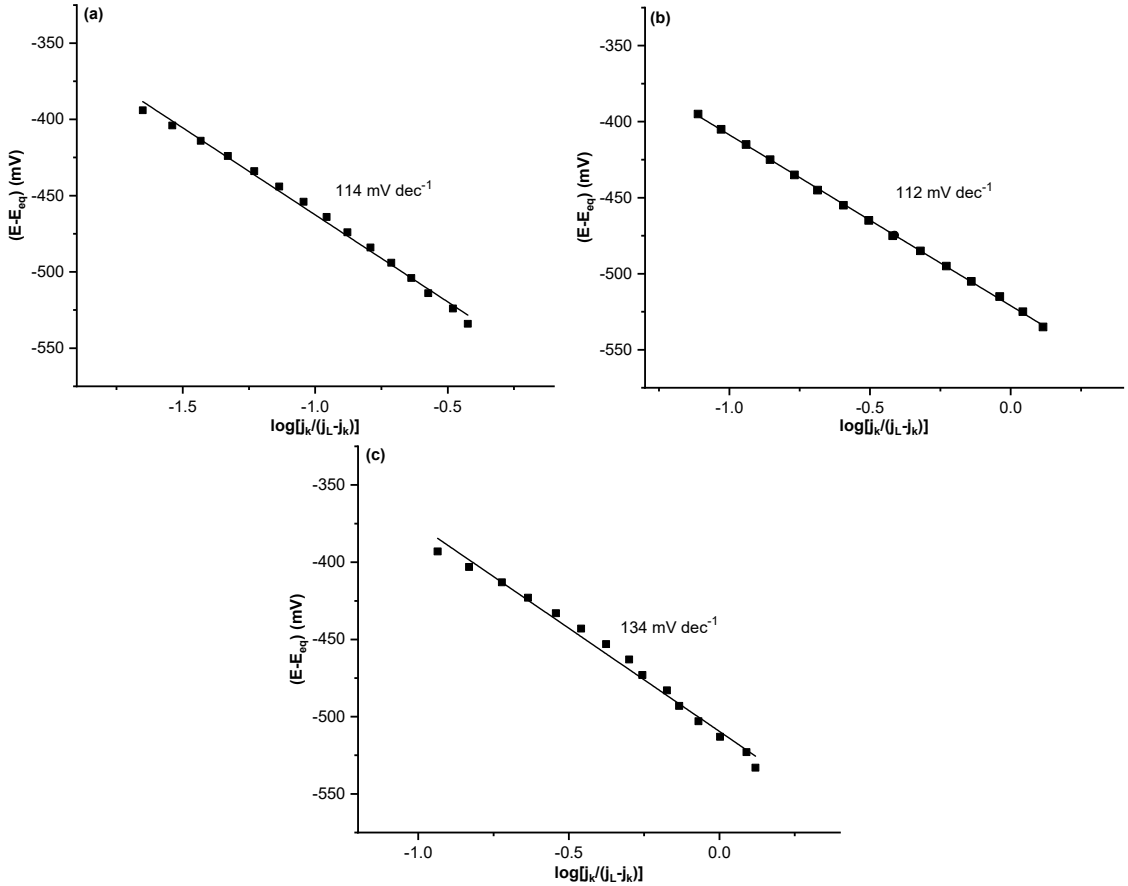

Fig 4. Relative Tafel plot for Pt/C in the solution of (a) H_2SO_4 0.5 M, (b) $HClO_4$ 0.1 M, and (c) NaOH 0.1 M

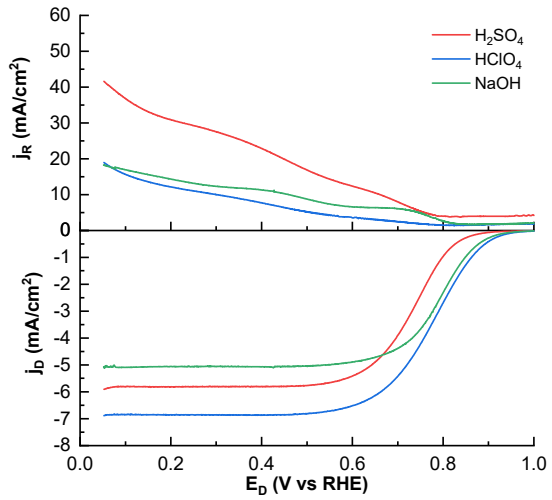

Fig 5. Polarization curves of RRDE for Pt/C in the different electrolyte solutions at 2500 rpm

yielded from the reduction of O_2. The smaller ring current means that the electron transfer is closer to 4. The polarization curve of RRDE can be used to determine the electron transfer number (as seen in Fig. 6) at a certain potential range with Eq. (5), where N is the collection efficiency (42%), I_D and I_R are disk and ring current, respectively.

$$n = \frac{4N|I_D|}{N|I_D| + I_R} = \frac{4}{1 + \frac{I_R}{N|I_D|}} \leq 4 \quad (5)$$

The value of n electron transfer in the electrolyte of $HClO_4$ 0.1 M was the closest to 4 and also the most stable as well, followed by NaOH 0.1 M and H_2SO_4 0.5 M. The result was similar to what Garsany et al. [20] reported. They reported that the electrocatalytic properties of Pt in the media of H_2SO_4 is sensible due to its surface in adsorbing HSO_4^- and SO_4^{2-} and the best performance of Pt/C is in the electrolyte of $HClO_4$ 0.1 M. The effect of the electrocatalyst performance was dependent on the electrolyte having interactions that occur between oxygen, salt ion, water, and the electrode. Electrolytes with

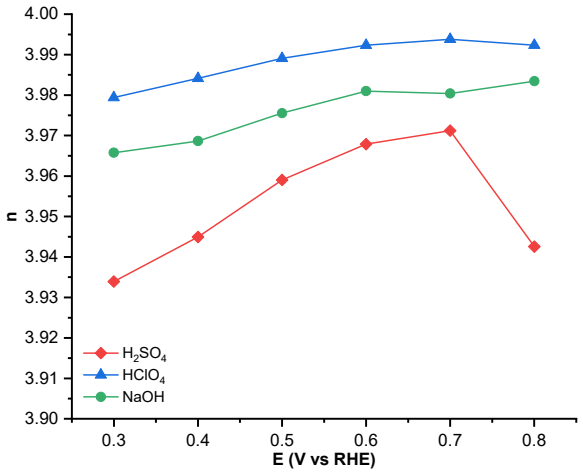

Fig 6. The electron transfer number for Pt/C in the different mediums at the potential range 0.8–0.3 V vs RHE

high O_2 saturation, lower viscosity, and weaker adsorption species increase the activity of ORR [21]. For example, the strongest adsorption is in H_2SO_4, and the weakest adsorption is in the solution of $HClO_4$ [22].

Tables 3 to 5 shows the result of the Pt/C test in the various electrolytes compared to the literature. The resulting test in our study was close to the literature. The slight difference between our test and the literature was due to a slightly different loading on the GC surface. In general, the test of the cell system obtained from this study was quite good. Therefore, the system we used is quite reliable with good confidence in determining unknown electrocatalysts from a sample.

The Electrocatalytic Performance of [Tb(TPP)(cyclen)]Cl

The measurement of the sample of [Tb(TPP)(cyclen)]Cl was conducted using the RRDE method at the potential range of 1.03 to 0.05 V vs RHE with the scanning rate of 5 mV/s and rotation rate of 200, 400, 900, 1600 and 2500 rpm to obtain the polarization curve in the O_2 saturated solution of NaOH 0.1 M. This choice of solution was considered due to the best stability of the sample in the alkaline media. Besides, in the alkaline media, the rate of the oxygen reduction reaction is faster [17]. The current obtained from the measurement was normalized with a surface (S_g) of about 0.126 cm^2. Fig. 7 shows the voltammetry profile of [Tb(TPP)(cyclen)]Cl in O_2 saturated electrolyte solution, in which the current density increases with the increase of rotation rate from 200 to 2500 rpm, similar to the Pt/C standard. Table 6 shows the E_{onset}, $E_{1/2}$, η, η (exp), and sluggishness of the polarization curve at 2500 rpm of the drop casted sample of [Tb(TPP)(cyclen)]Cl. [Tb(TPP)(cyclen)]Cl showed lower E_{onset} and $E_{1/2}$ values than Pt/C in the electrolyte solution. This indicated that [Tb(TPP)(cyclen)]Cl had less catalytic activity than Pt/C. Theoretically, the E_{onset} and $E_{1/2}$ that represent the electrocatalysis activity showed that [Tb(TPP)(cyclen)]Cl was 2.16 times slower than Pt/C.

The linearity of the Koutecky-Levich plot was quite good for [Tb(TPP)(cyclen)]Cl (see Fig. 8). Kinetic current

Table 3. The comparison of the test of Pt/C standard in H_2SO_4 0.5 M and the literature

Electrolyte of 0.5 M H_2SO_4	Pt loading ($\mu g_{Pt}/cm^2$)	E_{onset} (V vs RHE)	$E_{1/2}$ (V vs RHE)
In this study	31.8	0.84	0.74
Sun et al. [23]	19.4	0.95	0.78

Table 4. The comparison of the test of Pt/C standard in $HClO_4$ 0.1 M and the literature

Electrolyte of 0.1 M $HClO_4$	Pt loading ($\mu g_{Pt}/cm^2$)	E_{onset} (V vs RHE)	$E_{1/2}$ (V vs RHE)	n, 0.5 V vs RHE	j_l^{diff} (mA/cm^2), 1600 rpm
In this study	31.8	0.89	0.78	3.99	5.68
Wu et al. [24]	30	0.86	0.78	3.96	5.37

Table 5. The comparison of the test of Pt/C standard in NaOH 0.1 M and in the literature

Electrolyte of 0.1 M NaOH	Pt loading ($\mu g_{Pt}/cm^2$)	E_{onset} (V vs RHE)	$E_{1/2}$ (V vs RHE)	n, 0.7 V vs RHE	j_l^{diff} (mA/cm^2), 1600 rpm
In this study	31.8	0.89	0.8	3.98	4.39
Holade et al. [25]	26	1.005	0.85	4	4.7

density (j_k) was normalized with the mass of [Tb(TPP)(cyclen)]Cl that was drop-casted on the surface disk (20 µg). The value of j_k at 0.8 V vs RHE for the catalytic activity of [Tb(TPP)(cyclen)]Cl was about 0.06 mA/cm^2 mg.

The plot was based on Eq (2) as shown in Fig. 9, in which the value of j_L was determined from the plot extrapolation. The value of j_L for [Tb(TPP)(cyclen)]Cl was about 0.52 mA/cm^2.

The Relative Tafel plot for [Tb(TPP)(cyclen)]Cl is shown in Fig. 10. Information about the value of the Tafel slope (b) and exchange current density (j_0) could be obtained from this plot. The b value obtained was about 117 mV/dec, close to 120 mV/dec, and the j_0 was about 4.30×10^{-7} mA/cm^2. The value of j_0 [Tb(TPP)(cyclen)]Cl was lower than Pt/C (4.92×10^{-3}). This means that with a similar overpotential, the increase of the current density of [Tb(TPP)(cyclen)]Cl was much lower, and the kinetic charge exchange occurred very slowly.

The polarization curve of RRDE (Fig. 11) showed the current on the disk and the ring. The electron number at a certain potential range was obtained from the data of the polarization curve of RRDE using Eq. (5). The result of the n electron transfer number is shown in Fig. 12. [Tb(TPP)(cyclen)]Cl showed a fairly stable n electron transfer curve at a certain range of potentials. The n electron transfer increased with the decrease of the average potential at about 2.38. This result was still an inferior value compared to the n-transfer electron ideal, such as Pt at about 4. This result also indicated that

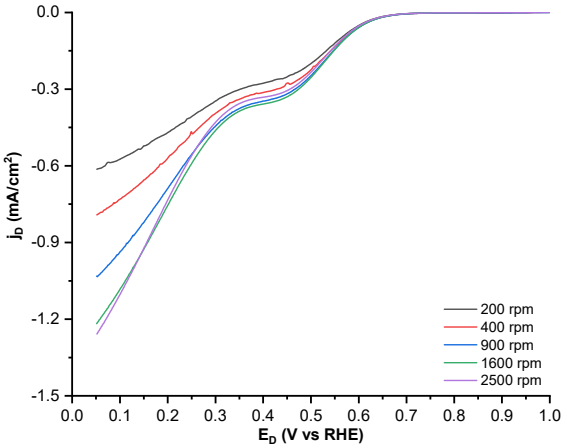

Fig 7. Polarization curve of [Tb(TPP)(cyclen)]Cl in the electrolyte of NaOH 0.1 M in the different rotation rates

Table 6. Parameter of polarization curve for [Tb(TPP)(cyclen)]Cl and comparison with Pt/C

Electrocatalyst	E_{onset} (V vs RHE)	$E_{1/2}$ (V vs RHE)	η (mV)	$\eta_{(exp)}$ (mV)	Sluggishness (mV)
[Tb(TPP)(cyclen)]Cl	0.62	0.53	283	558	275
Pt/C 20%	0.89	0.80	167	296	129

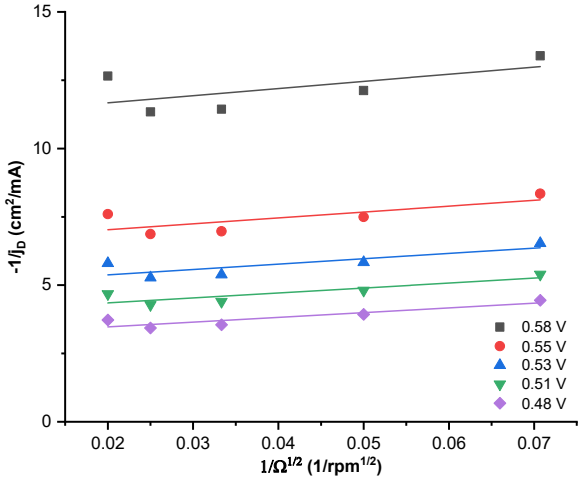

Fig 8. Koutecky-Levich plot determined from Fig. 7 for [Tb(TPP)(cyclen)]Cl in NaOH 0.1 M solution

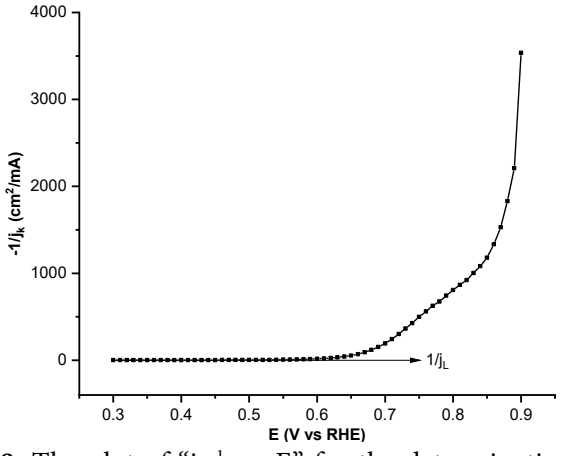

Fig 9. The plot of "j_k^{-1} vs. E" for the determination of limiting current density (j_L) for [Tb(TPP)(cyclen)]Cl in NaOH 0.1 M solution.

the ORR mechanism of [Tb(TPP)(cyclen)]Cl was via the (2 + 2) mechanism, where O_2 was first reduced to H_2O_2, followed by the reduction of H_2O_2 to H_2O.

The resume test result of [Tb(TPP)(cyclen)]Cl in the NaOH 0.1 M solution is shown in Table 7. The kinetic parameter of [Tb(TPP)(cyclen)]Cl was not ideal compared to Pt/C. This indicated that [Tb(TPP)(cyclen)]Cl was inappropriate material for the electrocatalysis of ORR. Some literature reported that this compound was mostly used for the magnetism application.

The catalytic performance of [Tb(TPP)(cyclen)]Cl can be explained by its structure energy level. Zhang and Xia [26] explained that the separation energy of the highest occupied molecular orbital (HOMO) and the lowest unoccupied molecular orbital (LUMO) could be used as a simple kinetic stability indicator. The low energy band gap of HOMO-LUMO indicated low kinetic stability and high chemical reactivity. The low HOMO-LUMO energetically was advantageous to increase the electron for high-lying LUMO and to extract electrons from low-lying HOMO. When comparing to the FePc (Fe-phthalocyanine) from Ma et al. [27], it can be seen that FePc owed the lower HOMO-LUMO gap with better electrocatalytic performance compared to [Tb(TPP)(cyclen)]Cl (Fig. 13). The E_{onset} and j_k are shown in Table 8. The lower value of E_{onset} and j_k indicated that the electrocatalytic performance of [Tb(TPP)(cyclen)]Cl was not better than FePc.

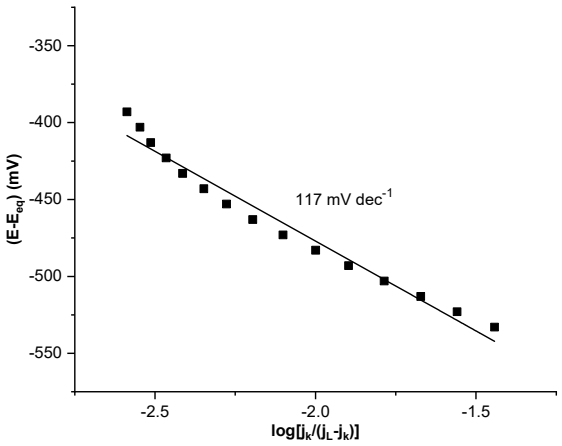

Fig 10. Relative Tafel plot for [Tb(TPP)(cyclen)]Cl in NaOH 0.1 M solution

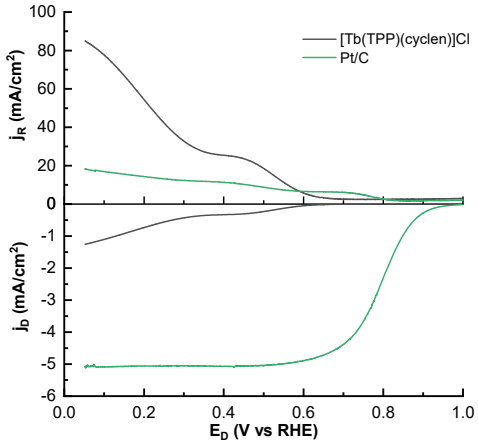

Fig 11. Polarization curve of RRDE for [Tb(TPP)(cyclen)]Cl and its comparison to Pt/C in the NaOH 0.1 M electrolyte at 2500 rpm

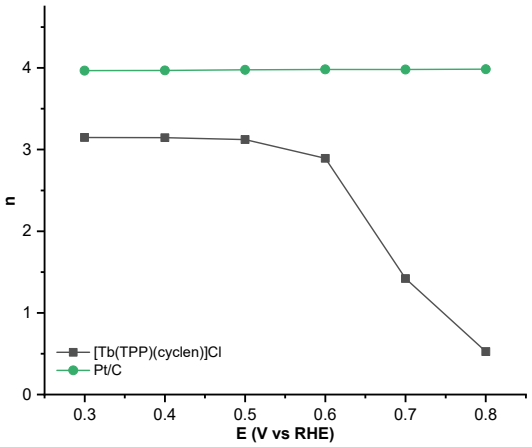

Fig 12. The n electron number of [Tb(TPP)(cyclen)]Cl and its comparison to Pt/C in NaOH 0.1 M solution at potential range of 0.8–0.3 V vs RHE

Table 7. Kinetic parameter of ORR of [Tb(TPP)(cyclen)]Cl and its comparison towards Pt/C

Electrocatalyst	n	j_k (mA/cm^{2}mg) at 0.8 V vs. RHE	j_L (mA/cm^2)	B (mV/dec)	j_0 (mA/cm^2)
[Tb(TPP)(cylene)]Cl	2.38	0.06	0.52	117	4.30×10^{-7}
Pt/C 20%	3.98	132.79	32.03	134	4.92×10^{-3}

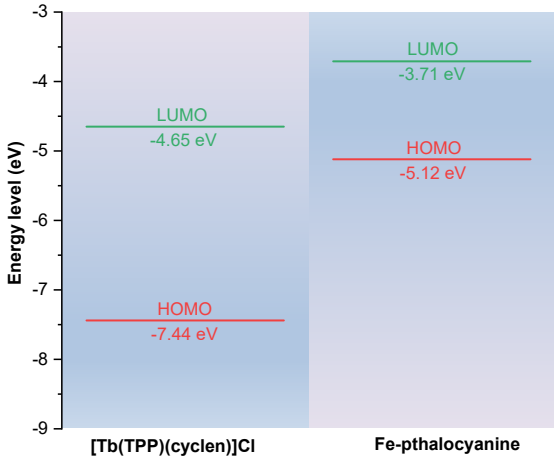

Fig 13. [Tb(TPP)(cyclen)]Cl and FePc energy level comparison

Table 8. Comparison of [Tb(TPP)(cyclen)]Cl and FePc

	[Tb(TPP)(cyclen)]Cl	FePc [27]
HOMO (eV)	-7.44	-5.12
LUMO (eV)	-4.65	-3.71
HOMO-LUMO gap (eV)	2.79	1.41
E_{onset} (V vs RHE)	0.62	0.958
j_k at 0.9 V (mA/cm^2)	2.83×10^{-4}	1.417

■ CONCLUSION

In the different electrolyte solutions, the Pt/C standard showed good results with an almost similar parameter value according to the literature (n close to 4). Meanwhile, the [Tb(TPP)(cyclen)]Cl sample was not a superior material for ORR electrocatalysis with an n electron transfer number of about 2.38. The result met the theoretical calculation of the HOMO-LUMO gap using DFT of about 2.79 eV, almost double to FePc (1.41 eV).

■ ACKNOWLEDGMENTS

This work was partly achieved through the use of Supercomputer System SQUID at the Cybermedia Center, Osaka University.

■ REFERENCES

[1] Özgür, T., and Yakaryılmaz, A.C., 2018, A review: Exergy analysis of PEM and PEM fuel cell based CHP systems, *Int. J. Hydrogen Energy*, 43 (38), 17993–18000.

[2] Park, K.Y., Sweers, M.E., Berner, U., Hirth, E., Downing, J.R., Hui, J., Mailoa, J., Johnston, C., Kim, S., Seitz, L.C., and Hersam, M.C., 2022, Mitigating Pt loss in polymer electrolyte membrane fuel cell cathode catalysts using graphene nanoplatelet pickering emulsion processing, *Adv. Funct. Mater.*, 32 (43), 2205216.

[3] Gewirth, A.A., Varnell, J.A., and DiAscro, A.M., 2018, Nonprecious metal catalysts for oxygen reduction in heterogeneous aqueous systems, *Chem. Rev.*, 118 (5), 2313–2339.

[4] Liu, M., Zhao, Z., Duan, X., and Huang, Y., 2019, Nanoscale structure design for high-performance Pt-based ORR catalysts, *Adv. Mater.*, 31 (6), 1802234.

[5] Lv, H., Guo, H., Guo, K., Lei, H., Zhang, W., Zheng, H., Liang, Z., and Cao, R., 2021, Substituent position effect of Co porphyrin on oxygen electrocatalysis, *Chin. Chem. Lett.*, 32 (9), 2841–2845.

[6] Liu, L., Ma, M., Xu, H., Yang, X., Lu, X., Yang, P., and Wang, H., 2022, S-doped M-N-C catalysts for the oxygen reduction reaction: Synthetic strategies, characterization, and mechanism, *J. Electroanal. Chem.*, 920, 116637.

[7] Zhou, Y., Xing, Y.F., Wen, J., Ma, H.B., Wang, F.B., and Xia, X.H., 2019, Axial ligands tailoring the ORR activity of cobalt porphyrin, *Sci. Bull.*, 64 (16), 1158–1166.

[8] Li, Y., Wang, N., Lei, H., Li, X., Zheng, H., Wang, H., Zhang, W., and Cao, R., 2021, Bioinspired N_4-metallomacrocycles for electrocatalytic oxygen reduction reaction, *Coord. Chem. Rev.*, 442, 213996.

[9] Liang, Z., Wang, H.Y., Zheng, H., Zhang, W., and Cao, R., 2021, Porphyrin-based frameworks for oxygen electrocatalysis and catalytic reduction of carbon dioxide, *Chem. Soc. Rev.*, 50 (4), 2540–2581.

[10] Santria, A., Fuyuhiro, A., Fukuda, T., and Ishikawa, N., 2017, Synthesis of a series of heavy lanthanide (III) monoporphyrinato complexes with tetragonal symmetry, *Inorg. Chem.*, 56 (17), 10625–10632.

[11] Shao, M., Chang, Q., Dodelet, J.P., and Chenitz, R., 2016, Recent advances in electrocatalysts for oxygen reduction reaction, *Chem. Rev.*, 116 (6), 3594–3657.

[12] Ruan, M., Liu, J., Song, P., and Xu, W., 2022, Meta-analysis of commercial Pt/C measurements for oxygen reduction reactions *via* data mining, *Chin. J. Catal.*, 43 (1), 116–121.

[13] Dolg, M., Stoll, H., and Preuss, H., 1989, Energy-adjusted *ab initio* pseudopotentials for the rare earth elements, *J. Chem. Phys.*, 90 (3), 1730–1734.

[14] Grimme, S., Antony, J., Ehrlich, S., and Krieg, H., 2010, A consistent and accurate *ab initio* parametrization of density functional dispersion correction (DFT-D) for the 94 elements H-Pu, *J. Chem. Phys.*, 132 (15), 154104.

[15] Petersson, G.A., and Al-Laham, M.A., 1991, A complete basis set model chemistry. II. Open-shell systems and the total energies of the first-row atoms, *J. Chem. Phys.*, 94 (9), 6081–6090.

[16] Wang, Q., Guesmi, H., Tingry, S., Cornu, D., Holade, Y., and Minteer, S.D., 2022, Unveiling the pitfalls of comparing oxygen reduction reaction kinetic data for Pd-based electrocatalysts without the experimental conditions of the current–potential curves, *ACS Energy Lett.*, 7 (3), 952–957.

[17] Mukherjee, M., Samanta, M., Ghorai, U.K., Murmu, S., Das, G.P., and Chattopadhyay, K.K., 2018, One pot solvothermal synthesis of ZnPc nanotube and its composite with RGO: A high performance ORR catalyst in alkaline medium, *Appl. Surf. Sci.*, 449, 144–151.

[18] Hebié, S., Bayo-Bangoura, M., Bayo, K., Servat, K., Morais, C., Napporn, T.W., and Boniface Kokoh, K., 2016, Electrocatalytic activity of carbon-supported metallophthalocyanine catalysts toward oxygen reduction reaction in alkaline solution, *J. Solid State Electrochem.*, 20 (4), 931–942.

[19] Napporn, T.W., Holade, Y., Kokoh, B., Mitsushima, S., Mayer, K., Eichberger, B., and Hacker, V., 2018, "Electrochemical Measurement Methods and Characterization on the Cell Level" in *Fuel Cells and Hydrogen*, Eds. Hacker, V., and Mitsushima, S., Elsevier, Amsterdam, Netherlands, 175–214.

[20] Garsany, Y., Baturina, O.A., Swider-Lyons, K.E., and Kocha, S.S., 2010, Experimental methods for quantifying the activity of platinum electrocatalysts for the oxygen reduction reaction, *Anal. Chem.*, 82 (15), 6321–6328.

[21] Jin, W., Du, H., Zheng, S., Xu, H., and Zhang, Y., 2010, Comparison of the oxygen reduction reaction between NaOH and KOH solutions on a Pt electrode: The electrolyte-dependent effect, *J. Phys. Chem. B*, 114 (19), 6542–6548.

[22] Wang, X., Li, Z., Qu, Y., Yuan, T., Wang, W., Wu, Y., and Li, Y., 2019, Review of metal catalysts for oxygen reduction reaction: From nanoscale engineering to atomic design, *Chem*, 5 (6), 1486–1511.

[23] Sun, T., Wu, Q., Che, R., Bu, Y., Jiang, Y., Li, Y., Yang, L., Wang, X., and Hu, Z., 2015, Alloyed Co–Mo nitride as high-performance electrocatalyst for oxygen reduction in acidic medium, *ACS Catal.*, 5 (3), 1857–1862.

[24] Wu, Z.S., Chen, L., Liu, J., Parvez, K., Liang, H., Shu, J., Sachdev, H., Graf, R., Feng, X., and Müllen, K., 2014, High-performance electrocatalysts for oxygen reduction derived from cobalt porphyrin-based conjugated mesoporous polymers, *Adv. Mater.*, 26 (9), 1450–1455.

[25] Holade, Y., Servat, K., Napporn, T.W., and Kokoh, K.B., 2015, Electrocatalytic properties of nanomaterials synthesized from "bromide anion exchange" method - Investigations of glucose and glycerol oxidation, *Electrochim. Acta*, 162, 205–214.

[26] Zhang, L., and Xia, Z., 2011, Mechanisms of oxygen reduction reaction on nitrogen-doped graphene for fuel cells, *J. Phys. Chem. C*, 115 (22), 11170–11176.

[27] Ma, Y., Li, J., Liao, X., Luo, W., Huang, W., Meng, J., Chen, Q., Xi, S., Yu, R., Zhao, Y., Zhou, L., and Mai, L., 2020, Heterostructure design in bimetallic phthalocyanine boosts oxygen reduction reaction activity and durability, *Adv. Funct. Mater.*, 30 (50), 2005000.